Quantum theory of spin waves in finite chiral spin chains

A. Roldán-Molina
Instituto de Física, Pontificia Universidad Católica de Valparaíso, Avenida Brasil 2950, Casilla 4059, Valparaíso, Chile

M. J. Santander and Á. S. Núñez
Departamento de Física, Facultad de Ciencias Físicas y Matemáticas, Universidad de Chile, Casilla 487-3, Santiago, Chile

J. Fernández-Rossier*
International Iberian Nanotechnology Laboratory, Av. Mestre Jose Veiga, 4715-310 Braga, Portugal
(Received 21 October 2013; revised manuscript received 6 January 2014; published 5 February 2014)

We calculate the effect of spin waves on the properties of finite-size spin chains with a chiral spin ground state observed on biatomic Fe chains deposited on iridium(001). The system is described with a Heisenberg model supplemented with a Dzyaloshinskii-Moriya coupling and a uniaxial single ion anisotropy that presents a chiral spin ground state. Spin waves are studied using the Holstein-Primakoff boson representation of spin operators. Both the renormalized ground state and the elementary excitations are found by means of Bogoliubov transformation, as a function of the two variables that can be controlled experimentally, the applied magnetic field and the chain length. Three main results are found. First, because of the noncollinear nature of the classical ground state, there is a *significant* zero-point reduction of the ground-state magnetization of the spin spiral. Second, there is a critical external field from which the ground state changes from chiral spin ground state to collinear ferromagnetic order. The character of the two lowest-energy spin waves changes from edge modes to confined bulk modes over this critical field. Third, in the spin-spiral state, the spin-wave spectrum exhibits oscillatory behavior as function of the chain length with the same period of the spin helix.

DOI: 10.1103/PhysRevB.89.054403 PACS number(s): 74.50.+r, 03.75.Lm, 75.30.Ds

I. INTRODUCTION

Because of the possibility of engineering and probing spin chains, atom by atom, using scanning tunneling microscope (STM) [1–6], the study of spin chains is not only a crucial branch in the study strong correlations and quantum magnetism [7,8] but also a frontier in the research of atomic scale spintronics [9]. Spin chains display a vast array of different magnetic states depending on the interplay between spin interactions, size of the chain, and their dissipative coupling to the environment. Thus, experiments reveal that different spin chains can behave like quantum antiferromagnets [1], classical antiferromagnets [3,6], and classical spin spirals [4]. When quantum fluctuations do not quench the atomic magnetic moment, classical information can be stored and manipulated in atomically engineered spin chains. Thus, classical Néel states can be used to store a bit of information [6] and the implementation of the NAND gate with two antiferromagnetic spin chains [3] have been demonstrated.

Spin waves are relevant excitations in systems that display a ground state with well-defined atomic spin magnetic moments, such as ferromagnets, antiferromagnetic Néel states, spin-spiral states, and skyrmions. Here we study the spin waves of finite-size spin chains that present a classical spin-spiral ground state. Spin waves have been studied in a variety of finite-size systems, including spin chains with ferromagnetic and antiferromagnetic ground states [10,11], as well as in skyrmions [12]. Our work is motivated by the recent experimental observation of a stabilized noncollinear chiral ground states in chains of Fe pairs deposited on Ir(001) [4] (see Fig. 1). This system [13] has attracted interest both because of the nontrivial interplay between structure and magnetic coupling [14,15] and because a local perturbation in one side of the chain affects the spin state globally, as a consequence of long range spin order [16], as in the case of antiferromagnetically coupled spin chains [3]. The robustness of spin spiral states against formation of domain walls is also considered an advantage [4].

Our interest on the spin waves in this system is twofold. First, spin excitations of spin chains, including spin waves, could be probed by means of inelastic electron tunneling spectroscopy (IETS) [1,17–19], which would provide an additional experimental characterization of the system, complementary to spin-polarized magnetometry [20]. Second, spin waves are a source of quantum noise that sets a limit to the capability of sending spin information along the chain.

The rest of this paper is organized as follows. In Sec. II we briefly discuss the fundamentals of the spin-spiral state ground state and the Hamiltonian used to describe it. In Sec. III we discuss the method to compute the spin-wave excitations. In Sec. IV we present the results of our numerical calculations. In Sec. V we summarize our main conclusions.

II. SPIN-SPIRAL HAMILTONIAN

Short-range isotropic Heisenberg exchange naturally yields collinear spin alignments, either ferro or antiferromagnetic. The competition with a spin coupling that promotes perpendicular alignment, such as the antisymmetric Dzyaloshinskii-Moriya (DM) interaction [21,22], $E_{\mathrm{DM}} = \sum_{i,j} \mathbf{D}_{i,j} \cdot (\mathbf{S}_i \times \mathbf{S}_j)$, naturally results in a noncollinear spin alignment between first neighbors in the plane normal to $\mathbf{D}_{i,j}$. In one-dimensional

*Permanent address: Departamento de Física Aplicada, Universidad de Alicante.

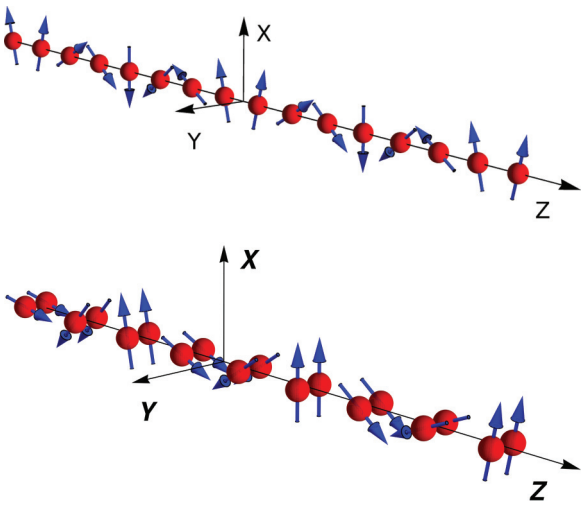

FIG. 1. (Color online) Schematic classical ground state for the mono strand (top) and the diatomic (bottom) chains. The parameters used in the calculation are given in the text. In both cases a magnetic field of 2T along the (1,0,0) direction is applied.

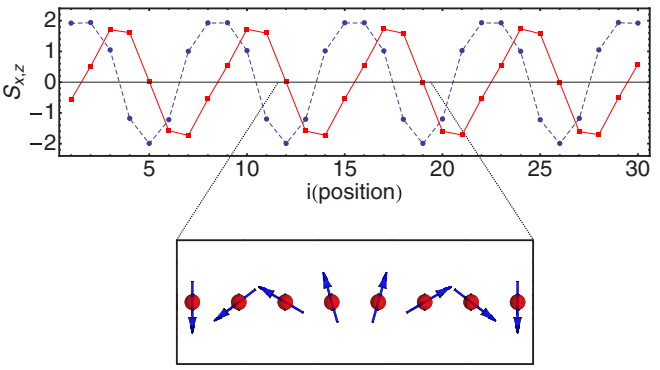

FIG. 2. (Color online) Projections of the classical ground state $\vec{\Omega}_i$ over the $\hat{x}$ (dashed blue) and the $\hat{z}$ (solid red) directions for the monostrand chain with first nearest-neighbor interactions. In this case we take $B = 1T$, $J = D = 1$ meV.

systems, the DM term leads to a spin-spiral states and in two dimensions promotes the formation of skyrmions [23]. For the spin chains considered here, the vector $\mathbf{D}_{i,j} = (0, D, 0)$ is the same for all couplings and lies along the $\hat{y}$ direction, perpendicular to the chain axis $\hat{z}$ (see Fig. 1). In these situations, any global rotation of the spin spiral in the (xz) plane would result in a state with the same energy. This large degeneracy is broken by the presence of single ion uniaxial anisotropy term that results in a preferred axis so there are only two classical ground states. In addition, the uniaxial anisotropy term distorts the spiral, preventing a uniform rotation angle along the chain. Finally, the application of a magnetic field $\mathbf{B}$ along the $\hat{x}$ direction (perpendicular both to the chain axis and to $\vec{D}$) can further break the symmetry, resulting in a unique ground state. These four terms are included in the Hamiltonian:

$$H = -\sum_{\langle i,j\rangle} J_{i,j}\mathbf{S}_i \cdot \mathbf{S}_j + \sum_{\langle i,j\rangle} \mathbf{D}_{i,j} \cdot (\mathbf{S}_i \times \mathbf{S}_j) + g\mu_B \mathbf{B} \cdot \sum_i \mathbf{S}_i - K \sum_i \left(S_i^x\right)^2. \quad (1)$$

We study two types of chains. First we consider a toy model of a mono strand chain, with first neighbor couplings only, $S = 2$, $D = J = 1$ meV, and $K = 2$ meV. Then we move to a more realistic description of the biatomic Fe chains [4] that includes couplings up to sixth neighbors, obtained from DFT calculations. In both cases the classical ground state is calculated by minimizing the energy as a function of the magnetic configuration, defined by the orientation of the magnetic moments $\vec{S}_i$, which are treated as classical vectors whose lengths remain fixed. The solutions are represented in the Figs. 1 and 2.

III. CALCULATION OF SPIN WAVES

The exact numerical diagonalization of the Hamiltonian (1), which would yield the spin excitations, is only possible in systems with a small number of atoms. Therefore, we use the spin-wave approximation. The calculation of the spin-wave spectrum of the finite-size chains is based on the representation of the spin operators in terms of Holstein Primakoff (HP) bosons [8,24] as follows:

$$\mathbf{S}_i \cdot \vec{\Omega}_i = S - a_i^\dagger a_i, \quad (2)$$

$$S_i^+ = \sqrt{2S - n_i}\, a_i, \quad (3)$$

$$S_i^- = a_i^\dagger \sqrt{2S - n_i}, \quad (4)$$

where $\vec{\Omega}_i$ is the spin direction of the classical ground state on the position i, $a_i^\dagger$ is a bosonic creation operator, and $n_i = a_i^\dagger a_i$ is the boson number operator. The operator n_i measures the deviation of the system from the classical ground state.

The essence of the spin-wave calculation is to replace the spin operators in Eq. (1) by the HP representation and the truncation up to quadratic order in the bosonic operators. Terms linear in the bosonic operators vanish when the expansion is done around the correct classical ground state. This approach has been widely used in the calculations of spin waves for ferromagnetic and antiferromagnetic ground states [7,8]. A generalized technique for the HP approach in noncollinear systems has been developed [25]. After a lengthy calculation detailed in the next subsections, we obtain the following spin-wave Hamiltonian:

$$H_{\mathrm{SW}} = \sum_i m_i a_i^\dagger a_i + \mu_i a_i^\dagger a_i^\dagger + \mathrm{H.c.} + \sum_{\langle i,j\rangle} t_{i,j} a_i^\dagger a_j + \tau_{i,j} a_i^\dagger a_j^\dagger + \mathrm{H.c.} \quad (5)$$

The specific values of elements $t_{i,j}$, $\tau_{i,j}$, m_i, and μ_i in the spin-wave Hamiltonian depend on the parameters of the interactions explicitly and implicitly by the classical ground state in the corresponding sites. In the case of a collinear ferromagnetic ground state, the anomalous terms that do not conserve the boson number vanish: $\tau_{i,j} = \mu_i = 0$. In general, in a noncollinear ground state, the anomalous terms differ from zero and the magnon number is no longer a conserved quantity. In these cases a Bogoliubov approach is needed in order to diagonalize the Hamiltonian. We undertake such task following the algorithm described in Ref. [26]. By so doing,

we can write the Hamiltonian (5) in the following form:

$$H_{\rm SW} = [\chi^\dagger\ \widetilde{\chi}]\bar{\mathbf{H}}\begin{bmatrix}\chi\\ \widetilde{\chi}^\dagger\end{bmatrix} - \frac{1}{2}{\rm Tr}[\bar{\mathbf{H}}], \tag{6}$$

where $\chi^\dagger = [a_1^\dagger\ \ a_2^\dagger \ldots a_N^\dagger]$. The Hermitian matrix $\bar{\mathbf{H}}$ is a $2N \times 2N$ Bogoliubov-de Gennes Hamiltonian that must be diagonalized in terms of paraunitary transformation matrix [26] $\mathcal{T}$. This yields the following diagonal form:

$$H_{\rm SW} = [\zeta^\dagger\ \widetilde{\zeta}]\frac{1}{2}\begin{bmatrix}\bar{\omega} & 0_{N\times N}\\ 0_{N\times N} & \bar{\omega}\end{bmatrix}\begin{bmatrix}\zeta\\ \widetilde{\zeta}^\dagger\end{bmatrix}, \tag{7}$$

where $\bar{\omega}$ is a $N \times N$ diagonal matrix with the spin-wave spectrum ω_η and $\zeta^\dagger = [\alpha_1^\dagger\ \alpha_2^\dagger \cdots \alpha_N^\dagger]$ are the operators that create the corresponding spin-wave excitations. Their relation to the original HP bosons is

$$\begin{bmatrix}\zeta\\ \widetilde{\zeta}^\dagger\end{bmatrix} = \mathcal{T}\begin{bmatrix}\chi\\ \widetilde{\chi}^\dagger\end{bmatrix}. \tag{8}$$

Thus, the ground state is defined by $\alpha_j|{\rm GS}\rangle = 0$ for all j and, in general, is not the same as the classical ground state. For a given magnonic state $|\psi_\eta\rangle \equiv \alpha_\eta^\dagger|{\rm GS}\rangle$, the deviation from the classical ground state at site i is given by $\rho_{i,\eta} = \langle\psi_\eta|a_i^\dagger a_i|\psi_\eta\rangle$.

Importantly, this quantity is nonzero even in the ground state, $\rho_{i,{\rm GS}} = \langle{\rm GS}|a_i^\dagger a_i|{\rm GS}\rangle$, reflecting the zero-point quantum fluctuations that are a consequence of a noncollinear classical ground state and lead to a reduction of the magnetization along the classical direction [see Eq. (2)].

A. Holstein-Primakoff Hamiltonian in the noncollinear ground state

The HP representation of the spin operator discriminates one direction [see, for instance, Eq. (2)] which is normally given by the magnetization of the classical ground state. Here we describe the technical details related to the use of HP bosons to compute the effective Hamiltonian in the case of noncollinear classical ground states. For that matter, it is convenient to define a rotated local coordinate system as follows:

$$\begin{aligned}\hat{e}_i^1 &= \cos\theta_i\ \cos\phi_i\ \hat{x} + \cos\theta_i\ \sin\phi_i\ \hat{y} - \sin\theta_i\ \hat{z}\\ \hat{e}_i^2 &= \hat{e}_i^3 \times \hat{e}_i^1\\ \vec{\Omega}_i = \hat{e}_i^3 &= \sin\theta_i\ \cos\phi_i\ \hat{x} + \sin\theta_i\ \sin\phi_i\ \hat{y} + \cos\theta_i\ \hat{z}\end{aligned}$$

or, in a more compact form,

$$\hat{e}_\alpha^i = \left(R_{\alpha,\beta}^i\right)^{-1}\hat{r}^\beta, \tag{9}$$

where the angles θ_i and ϕ_i characterize the spin direction on the classical ground state in the site i and $\hat{r}^\beta$ are the Cartesian axis. In this framework, the Hamiltonian (1) is expressed as:

$$\begin{aligned}H_{\rm ex} &= \sum_{i,j} J_{i,j}\vec{S}_i\cdot\vec{S}_j\\ &= \sum_{i,j} J_{i,j}\left(\vec{S}_i\cdot\hat{e}_\alpha^i\right)\left(\vec{S}_j\cdot\hat{e}_\beta^j\right)R_{\alpha,\gamma}^i R_{\beta,\gamma}^j,\end{aligned} \tag{10}$$

$$\begin{aligned}H_{\rm DM} &= \sum_{i,j}\vec{D}_{i,j}\cdot\vec{S}_i\times\vec{S}_j\\ &= \sum_{i,j}\left(\vec{S}_i\cdot\hat{e}_\alpha^i\right)\left(\vec{S}_j\cdot\hat{e}_\beta^j\right)R_{\alpha,\gamma}^i\bar{D}_{i,j}^{\gamma,\eta}R_{\eta,\beta}^j,\end{aligned} \tag{11}$$

where we have defined $\bar{D}_{i,j}^{\gamma,\eta} \equiv D_{i,j}^a\epsilon_{\gamma,\eta,a}$ and $\epsilon_{\gamma,\eta,a}$ is the Levi-Civita symbol and a sum over repeated indexes is understood,

$$\begin{aligned}H_A &= -\sum_{i,\alpha}K_\alpha\left(S_i^\alpha\right)^2\\ &= -\sum_i\left(\vec{S}_i\cdot\hat{e}_\alpha^i\right)\left(\vec{S}_i\cdot\hat{e}_\beta^i\right)R_{\alpha,\gamma}^i\bar{K}_i^{\gamma,\eta}R_{\eta,\beta}^i,\end{aligned} \tag{12}$$

$$H_{\rm Zee} = \mu_s\sum_{i,\alpha}\vec{B}_i\cdot\vec{S}_i = \mu_s\sum_i\left(\vec{S}_i\cdot\hat{e}_\alpha^i\right)R_{\alpha,\gamma}^i B_i^\gamma. \tag{13}$$

In the specific case considered here, where $\vec{D}_{i,j} \parallel \hat{y}$ and $\hat{x}$ direction as anisotropic easy axis, we have the following:

$$\bar{D}_{i,j}^{\gamma,\eta} = D_{i,j}(\delta_{\gamma,3}\delta_{\eta,1} - \delta_{\gamma,1}\delta_{\nu,3}), \tag{14}$$

$$\bar{K}_i^{\gamma,\eta} = K_i\ \delta_{\gamma,1}\ \delta_{\eta,1}. \tag{15}$$

The derivation of the HP Hamiltonian of Eq. (5) starts with the combined use of Eq. (2) and the following expressions:

$$S_i^\pm = \vec{S}_i\cdot\hat{e}_1 \pm i\vec{S}_i\cdot\hat{e}_2, \tag{16}$$

$$S - n_i = \vec{S}_i\cdot\vec{\Omega}_i. \tag{17}$$

By inserting this in Eq. (10)–(13), and keeping up to second-order terms in the bosonic operators $a^\dagger$,a, we are able to write the effective spin-wave Hamiltonian in the form of Eq. (6), with

$$\bar{\mathbf{H}} = \begin{bmatrix}\mathbf{A} & \mathbf{B}\\ \mathbf{B}^* & \mathbf{A}^*\end{bmatrix}, \tag{18}$$

where $\mathbf{A}$ and $\mathbf{B}$ are $2N \times 2N$ hermitic and symetric matrix, respectively.

B. Specific Hamiltonian parameters for the chiral spin chain case

In the specific case of the diatomic chain, the elements of the matrices $\mathbf{A}$ and $\mathbf{B}$ read as follows:

$$\begin{aligned}A_{i,j} &= \delta_{i,j}\begin{bmatrix}m_i & t_p\\ t_p & m_i\end{bmatrix} + (1-\delta_{i,j})\begin{bmatrix}t_{i,j} & 0\\ 0 & t_{i,j}\end{bmatrix}\\ B_{i,j} &= \delta_{i,j}\begin{bmatrix}\mu_i & 0\\ 0 & \mu_i\end{bmatrix} + (1-\delta_{i,j})\begin{bmatrix}\tau_{i,j} & 0\\ 0 & \tau_{i,j}\end{bmatrix},\end{aligned}$$

where

$$\begin{aligned}m_i = \frac{S}{2}&\sum_{j=-6}^{6}(J_{i,i+j}\cos[\theta_i - \theta_{i+j}] + D_{i,i+j}\sin[\theta_i - \theta_{i+j}])\\ &+ \frac{1}{2}K(2S - 1 - (3S-2)\cos^2[\theta_i]) + \frac{h}{2}\sin[\theta_i]\\ &+ \frac{S}{2}J_p,\end{aligned} \tag{19}$$

TABLE I. Exchange and DM constants extracted from fits to the DFT calculations [4].

$\|i-j\|$	1	2	3	4	5	6
$J_{i,j}$(meV)	0.53	1.42	−0.12	−0.34	−0.29	0.37
$D_{i,j}$(meV)	2.58	−2.77	−0.07	0.63	−0.36	−0.12

where J_{ij} and D_{ij} stand for interdimer exchange and DM coupling, K arises from the unaxial single atom anisotropy and J_p stands for the intradimer ferromagnetic exchange. The values for J_{ij} and D_{ij} are given in Table I [4]. The other terms in matrices A and B are as follows:

$$\mu_i = -\frac{S}{2}K\sqrt{1+\frac{1}{2S}}\cos^2\theta_i$$
$$t_{i,j} = -\frac{1}{4}S(J_{i,j}(1+\cos[\theta_i-\theta_j]) + D_{i,j}\sin[\theta_i-\theta_j])$$
$$\tau_{i,j} = \frac{1}{4}S(J_{i,j}(1-\cos[\theta_i-\theta_j]) - D_{i,j}\sin[\theta_i-\theta_j])$$
$$t_p = -\frac{S}{2}J_p. \quad (20)$$

IV. RESULTS

We now apply the formalism of the previous section to compute the spin waves of finite-size chains with spin-spiral ground states. This method has been applied to infinite crystals, providing the spin-wave dispersion $\omega(q)$ associated to spin spirals [27].

A. First-nearest-neighbor interaction monostrand chain

We address first the case of a simple chain with first-nearest-neighbors exchange and DM interactions. In spite of its simplicity, we shall see that this simple model captures the essence of the physical behavior of the spin waves in the more realistic case described in the next subsection. The first step is to calculate the classical ground state. For a given choice of Hamiltonian parameters, the ground state is found either by use of a self-consistent minimization procedure or by use of a classical Monte Carlo. The ground state of the mono strand chain is shown Fig. 1(a) and also in Fig. 2, for uniaxial anisotropy $K = 2$ meV, $S = 2$, and $J = D = 1$ meV. It is apparent that, because of the single-ion anisotropy term, the spin spiral is distorted. The choice of $\vec{D} = (0, D, 0)$ yields a spin spiral in the xz plane. The period of the spiral is approximately seven atoms, slightly shorter than the result obtained from the case without anisotropy $[2\pi/\arctan(\frac{D}{J})]$.

Once the classical ground state is determined, the problem is reduced to diagonalize the Hamiltonian in Eq. (5). This is achieved using the Bogoliubov-de Gennes prescription described in the previous section. We focus on the spin-wave spectrum of finite-size chains with $N = 30$ sites. In Fig. 3(a), we show the evolution of the five lowest energy modes as a function of the applied field B, applied along the easy axis ($\hat{x}$). The abrupt change in the spectrum at fields near 2 T corresponds to a drastic modification of the ground state from helical to ferromagnetic order. This can be seen in Fig. 3(b),

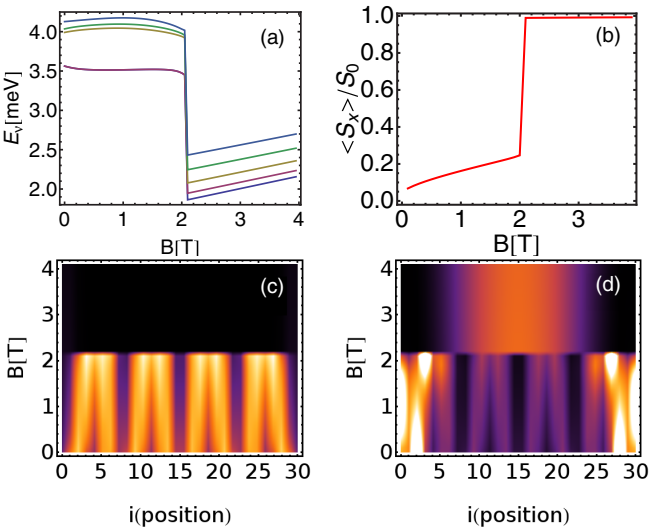

FIG. 3. (Color online) Magnonic excitation analysis for the monostrand nearest-neighbor interaction chain as a function of magnetic fields along the x axis. Energies for the first five excited states (a), dependence of the net spin along the x axis for the classical ground state (b), and magnonic occupation on the ground state (c) and the first excited state (d). In these plots, black stands for null $\langle a_i^\dagger a_i\rangle$ and white for maximal fluctuation.

where we show the dependence of the net magnetization along the x axis for the classical ground state as a function of field. The jump in the spin-wave spectrum takes place at the same field as the jump in the magnetization.

In Figs. 3(c) and 3(d) we show the expectation value of the HP boson occupation number $\langle a_i^\dagger a_i\rangle$ calculated within the spin-wave vacuum [Fig. 3(c)] and the lowest energy spin-wave state [Fig. 3(d)] as a function of both the applied field (vertical axis) and chain site (horizontal axis). The first thing to notice is that, in the spin-spiral state, the quantum spin fluctuations are present even in the ground state. These fluctuations disappear in the FM ground state. The ground-state fluctuations present an oscillation across the chain, commensurate with the spin spiral. The character of the first excited spin wave also changes from a edge mode in the spin spiral to a extended state with a magnon density proportional to $\sin[\pi\frac{i}{N}]$.

B. Real Fe biatomic chain on Ir(001)

We now compute the spin-wave spectrum of the biatomic Fe chains, described with a realistic spin Hamiltonian, obtained by fitting DFT calculations, further validated by comparison with the experimental observations [4]. The exchange and DM parameters so obtained include interactions up to the six nearest neighbors (see Table I). Interestingly, the results for the realistic model are qualitatively consistent with the findings of the simpler toy model of the previous subsection. We consider a chain with $N = 30$ Fe dimers.

The ferromagnetic coupling inside a given Fe dimer is denoted by $J_p = 160$ meV [4] and is the dominant energy scale in the problem. As a result, the spins in the dimer are parallel. The spin order along the chain is given by a spin spiral with period 3, as shown in Fig. 1(b).

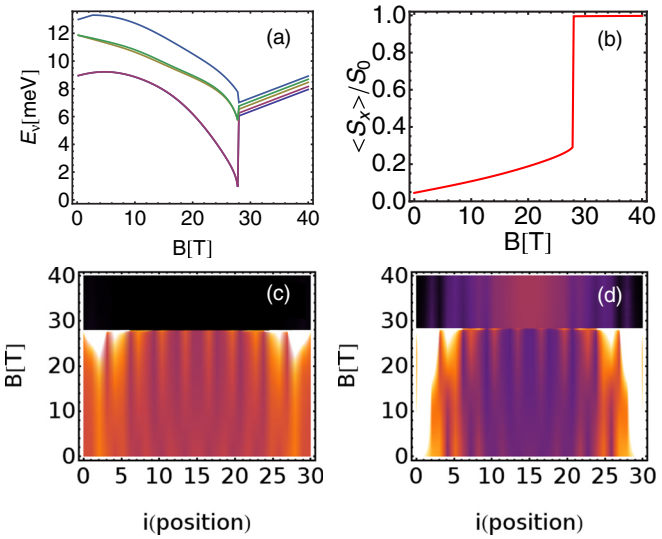

FIG. 4. (Color online) Magnonic excitation properties for a 30-site biatomic Fe chain on Ir(001) as a function of a magnetic field along the x axis. Energies for the first five excited states (a), dependence of the net spin along the x axis for the classical ground (b), and magnonic occupation on the ground state (c) and the first excited state (d). In these plots, black denotes null $\langle a_i^\dagger a_i \rangle$ and white denotes maximal fluctuation. Quantum fluctuations increase with the field in frustrated spin sites.

In analogy with the results of the previous subsection, in Fig. 4(a) we also show the evolution of the five lowest energy spin waves as a function of the applied magnetic field along the $\hat{x}$ direction. These modes evolve smoothly up to a critical field ($B \sim 28$T), where an abrupt change takes place, corresponding to a phase transition from the helical state to a collinear ferromagnetic ground state. This phase transition is also revealed in Fig. 4(b), where we show the total magnetization along the field direction as a function of the field strength. Our calculations show an abrupt change of behavior at the critical field.

In analogy with the results of the previous subsection, in Figs. 4(c) and 4(d) we show the expectation value of the HP boson occupation number $\langle a_i^\dagger a_i \rangle$ calculated within the spin-wave vacuum [Fig. 4(c)] and the lowest-energy spin-wave state [Fig. 4(d)] as a function of both the applied field and the chain site. In this case it is also true that quantum spin fluctuations are present even in the ground state and disappear in the FM ground state. The main differences between the two cases are the following. First, the modulation in the intensity of the quantum spin fluctuations across the chain have a different period that corresponds to the different wavelength of the spin spiral. Second, the quantum spin fluctuations of the spin-wave state in the FM state (at high field) have a fine structure, compared with their mono strand analog, which arises from the coupling beyond first neighbors.

We now discuss how the spin-wave spectrum depends on the other parameter that can be controlled experimentally, namely the number of dimers in the diatomic chain, N. In Fig. 5 we show the evolution of the six lowest spin-wave energies E_ν as a function of N for the spin-spiral state (left panel) and the ferromagnetic state (right panel). It is apparent that, for the

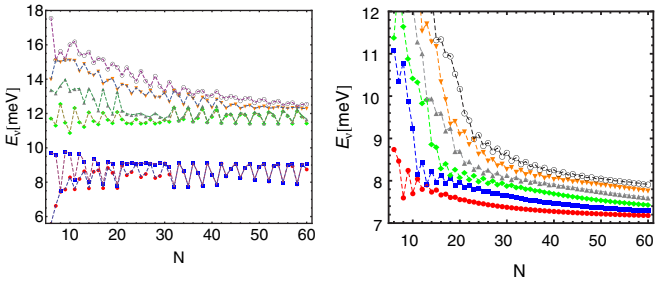

FIG. 5. (Color online) Six lowest-lying excitation energies as function of the chain's length for the spin spiral (left panel) and the ferromagnetic ground state (right panel). The calculation is 2T and 32T respectively.

spin spiral, the E_ν present oscillations commensurate with the period of the spin spiral (three dimers). The main reason for the oscillations in all the physical properties (both in the ground state and the excitation spectra) with the number of sites is related to the commensurability of the helix and the size of the chain. Since the helix period is three oscillations take place with period three. The plot of Fig. 4(d), together with the gap between these first two spin-wave energies and others as a function of N, suggest that they are edge modes. Their splitting at small N arises from the hybridization of the two edge modes. Therefore, a STM could excite more easily the system in this mode when acting upon the edge atoms (something similar has been reported in Ref. [19]). Future work will determine if this could result in an effective way to manipulate the spiral. In contrast, as soon as N is significantly larger than the range the exchange interactions, the evolution of the E_ν in the ferromagnetic case displays a monotonic decrease as a function of N, consistent with the picture of only confined bulk modes.

V. SUMMARY AND CONCLUSIONS

We have studied the effect of spin-wave excitations on the magnetic properties of finite-size spin spirals, as those observed in recent experiments [4]. We have considered both a simple model with one atom per unit cell and first-neighbor interactions as well as a more realistic [4] model with up to six neighbor couplings and two atoms in the unit cell. In both cases we find three interesting results. First, application of a magnetic field results in a phase transition from a spin-spiral state at low field to a ferromagnetic state above a critical field. Second, the spin-spiral ground state has zero-point fluctuations that induce a reduction of the magnetization. These zero-point fluctuations are absent in the ferromagnetic state. Third, the two lowest energy spin waves of the spin spiral are edge modes, in contrast to the bulk character of the spin waves in the ferromagnetic case.

Our findings could be verified by means of inelastic electron tunneling spectroscopy. The existence of edge modes might provide a tool to manipulate the spin spiral by means of selective excitation of edge atoms with STM.

ACKNOWLEDGMENTS

We acknowledge F. Delgado for fruitful discussions and careful reading of the manuscript. The authors

thank funding from grants from Fondecyt (Grant No. 1110271), Fondo de Innovación para la Competitividad-MINECON (Grant No. ICM P10-061-F), and Anillo ACT (Grant No. 1117). A.S.N. also acknowledges support from Financiamiento Basal para Centros Científicos y Tecnológicos de Excelencia under Project No. FB 0807 (Chile). A.R.M., M.J.S., and A.S.N. acknowledge the hospitality of the INL.

[1] C. F. Hirjibehedin *et al*., Science **312**, 1021 (2006).
[2] D. Serrate *et al*., Nat. Nanotechnol. **5**, 350 (2010).
[3] A. Khajetoorians *et al*., Science **332**, 1062 (2011).
[4] M. Menzel, Y. Mokrousov, R. Wieser, J. E. Bickel, E. Vedmedenko, S. Blügel, S. Heinze, K. von Bergmann, A. Kubetzka, and R. Wiesendanger, Phys. Rev. Lett. **108**, 197204 (2012).
[5] A. Khajetoorians *et al*., Nat. Phys. **8**, 497 (2012).
[6] S. Loth *et al*., Science **335**, 196 (2012).
[7] K. Yosida, *Theory of Magnetism* (Springer, Heidelberg, 1996).
[8] Assa Auerbach, *Interacting Electrons and Quantum Magnetism* (Springer, New York, 1994).
[9] J. Fernández-Rossier, Nat. Mat. **12**, 480 (2013).
[10] R. Wieser, E. Y. Vedmedenko, and R. Wiesendanger, Phys. Rev. Lett. **101**, 177202 (2008).
[11] R. Wieser, E. Y. Vedmedenko, and R. Wiesendanger, Phys. Rev. B **79**, 144412 (2009).
[12] S. Z. Lin, C. D. Batista, and A. Saxena, arXiv:1309.5168.
[13] L. Hammer, W. Meier, A. Schmidt, and K. Heinz, Phys. Rev. B **67**, 125422 (2003).
[14] R. Mazzarello and E. Tosatti, Phys. Rev. B **79**, 134402 (2009).
[15] Y. Mokrousov, A. Thiess, and S. Heinze, Phys. Rev. B **80**, 195420 (2009).
[16] S. Onoda, Physics **5**, 53 (2012).
[17] J. Fernández-Rossier, Phys. Rev. Lett. **102**, 256802 (2009).
[18] J. P. Gauyacq and N. Lorente, Phys. Rev. B **83**, 035418 (2011).
[19] F. Delgado, C. D. Batista, and J. Fernández-Rossier, Phys. Rev. Lett. **111**, 167201 (2013).
[20] R. Wiesendanger, Rev. Mod. Phys. **81**, 1495 (2009).
[21] I. Dzyaloshinsky, J. Phys. Chem. Solids **4**, 241 (1958).
[22] T. Moriya, Phys. Rev. **120**, 91 (1960).
[23] A. Fert, V. Cross, and J. Sampaio, Nat. Nano. **8**, 152 (2013).
[24] T. Holstein and H. Primakoff, Phys. Rev. **58**, 1098 (1940).
[25] J. T. Haraldsen and R. S. Fishman, J. Phys.: Condens. Matter **21**, 216001 (2009).
[26] J. H. P. Colpa, Physica A **93**, 327 (1978).
[27] A. Zheludev, S. Maslov, G. Shirane, I. Tsukada, T. Masuda, K. Uchinokura, I. Zaliznyak, R. Erwin, and L. P. Regnault, Phys. Rev. B **59**, 11432 (1999).